Pharmacogenomics and Personalized Medicine

Dovepress
Taylor & Francis Group

Open Access Full Text Article

ORIGINAL RESEARCH

Bioinformatic Identification and Preliminary Validation of TP53, TGFB1, and NFE2L2 as Potential Ferroptosis-Related Regulators in Pancreatic Adenocarcinoma

Shouying Li[1], Chunfang Zhang[1], Shengxiang Lv[1], Zhimei Zhang[1], Dazhou Xu[1], Tonglei Xu[1,2]

[1]Department of Gastroenterology and Department of Pathology, Lianyungang Clinical College of Nanjing Medical University/ The First People's Hospital of Lianyungang, Lianyungang, Jiangsu, People's Republic of China; [2]Department of Hepatobiliary and Pancreatic Surgery, Zhongda Hospital, Southeast University, Nanjing, People's Republic of China

Correspondence: Dazhou Xu; Tonglei Xu, Email Xdz928@163.com; 230239134@seu.edu.cn

Background: Pancreatic adenocarcinoma (PAAD) is a highly malignant tumor with very poor prognosis for patients. Ferroptosis, as a novel cell death mechanism, brings a new direction for PAAD therapeutic research.

Methods: Ferroptosis-related differentially expressed genes were identified by bioinformatic analysis of the FerrDb, TCGA, and GTEx databases. A series of analyses, including functional enrichment, protein-protein interaction (PPI) networking, survival analysis, and immune infiltration profiling, were performed to screen for and characterize hub genes. Subsequently, the expression of key hubs —NFE2L2 (NRF2), TGFB1, and TP53—was validated in PDAC patient tissues and cell lines using qRT-PCR and Western blot. Their biological functions were investigated via shRNA-mediated knockdown in BxPC-3 cells, followed by assays for cell migration (wound healing, transwell) and ferroptosis (ROS, MDA, GSH/GSSG).

Results: Bioinformatic analysis identified 221 ferroptosis-related DEGs. NFE2L2, TGFB1, and TP53 emerged as core hub genes whose high expression correlated with poor patient survival and specific immune infiltration patterns. Experimental validation confirmed that NRF2, TGFβ1, and TP53 proteins were significantly upregulated in PDAC tissues compared to adjacent normal tissues. Functionally, knockdown of NFE2L2 and TGFB1 suppressed PDAC cell migration, whereas TP53 knockdown enhanced it. Inversely, NFE2L2 knockdown promoted ferroptosis (increased ROS and MDA, decreased GSH), while knockdown of both TGFB1 and TP53 inhibited ferroptosis.

Conclusion: TP53, TGFB1, and NRF2 are key ferroptosis-related regulators in PAAD, influencing tumor progression, ferroptosis sensitivity, and immune contexture. These findings provide new insights and potential targets for ferroptosis-based therapies in PAAD.

Keywords: pancreatic adenocarcinoma, ferroptosis, PPI, hug genes, GEPIA

Introduction

Pancreatic adenocarcinoma (PAAD), one of the most lethal malignant tumors globally, has a dismal five-year survival rate of less than 10%, posing a substantial public health threat.[1] Its incidence is rising at 0.5–1.0% annually, with projections to become the second leading cause of cancer death in the US by 2030.[2] Pancreatic ductal adenocarcinoma (PDAC) accounts for up to 90% of pancreatic tumors, while other subtypes like follicular carcinomas, pancreatoblastomas, and neuroendocrine tumors are rare.[3] The high mortality rate of pancreatic adenocarcinoma is mainly attributed to its late diagnosis and the aggressiveness of the disease. Patients are often diagnosed when the disease has progressed to an advanced stage, with metastasis and high resistance to conventional therapies such as chemotherapy and radiotherapy.[4–15] Despite advances in imaging and surgery, overall prognosis remains poor, underscoring the urgent need for new therapies and deeper insights into its molecular drivers.[16] At the molecular level, PAAD is characterized by complex genomic alterations, including mutations in oncogenes (KRAS), tumor suppressor genes (TP53, CDKN2A), and tumor microenvironment aberrations, which enable

https://doi.org/10.2147/PGPM.S562602
Received: 22 August 2025
Accepted: 22 January 2026
Published: 17 February 2026

immune evasion, apoptosis resistance, and survival in nutrient-poor conditions.[15,17–19] In recent years, targeting tumor cell death mechanisms has emerged as a promising strategy to identify novel molecular targets.

Ferroptosis represents a distinct iron-dependent programmed cell death driven by intracellular iron accumulation and lipid peroxidation, differs from apoptosis, necrosis, or autophagy, which offering a new avenue for PAAD therapy.[20–22] PAAD cells exhibit high sensitivity to oxidative stress and metabolic perturbations in their microenvironment, making ferroptosis a viable therapeutic target.[23] Abnormal iron metabolism in PAAD cells such as reduced ferritin and increased iron transporter TfR1 promotes free iron accumulation and lipid peroxidation, while impaired glutathione (GSH) metabolism hinders lipid peroxidation clearance, accelerating ferroptosis.[24,25] These features provide a robust molecular basis for targeting ferroptosis in PAAD. Notably, ferroptosis acts as a key regulator of the PAAD tumor immune microenvironment. Ferroptotic cells release DAMPs to enhance dendritic cell activation and T cell infiltration, and ferroptosis-related genes modulate immune cell function, connecting ferroptosis to PAAD-relevant immune surveillance.[26]

However, critical knowledge gaps remain in translating ferroptosis research to PAAD. Firstly, the key ferroptosis-related regulators that drive PAAD progression, modulate ferroptosis sensitivity, and shape the immune microenvironment are not clearly defined, previous studies focused on individual genes rather than systematic identification of core hubs. Secondly, the functional crosstalk among ferroptosis regulators, PAAD cell migration, and immune infiltration has been rarely elucidated, which limits the understanding of how targeting ferroptosis can simultaneously address the issues of tumor growth and immune escape. Thirdly, while genes like TP53 (a tumor suppressor with reported ferroptosis regulatory roles), TGFB1 (a cytokine linked to PAAD metastasis), and NFE2L2 (a master antioxidant regulator) have been implicated in both ferroptosis and cancer, their coordinated roles in PAAD-specific ferroptosis and immune modulation remain uncharacterized.[27–29]

This study aims to integrate bioinformatics analysis and experimental validation to identify DEGs related to ferroptosis in PAAD, screen out core hub genes, and functionally characterize their roles in cell migration and ferroptosis. By focusing on TP53, TGFB1, and NFE2L2 as potential key regulatory factors, this study attempts to provide new molecular insights into the progression of pancreatic cancer and lay the foundation for ferroptosis-based therapeutic strategies.

Materials and Methods

Data Collection and Gene Identification

Ferroptosis-Related Gene Collection

Ferroptosis-related genes (FRGs) were obtained from FerrDb (http://www.zhounan.org/ferrdb/), a comprehensive database dedicated to ferroptosis regulators and associated diseases. Three datasets (Driver, Suppressor, and Marker) were downloaded, yielding 388 unique ferroptosis-related genes after duplicate removal.

PAAD Dataset Acquisition and Differential Expression Analysis Using R Software

Gene expression data for pancreatic adenocarcinoma (PAAD) were retrieved from GEPIA (http://gepia.cancer-pku.cn/), which integrates RNA sequencing data from The Cancer Genome Atlas (TCGA) and Genotype-Tissue Expression (GTEx) databases. The dataset comprised gene expression profiles from 179 PAAD tumor samples and 171 normal pancreatic tissue samples. Differential expression analysis was performed using the DESeq2 package (version 1.38.3) in R software (version 4.2.1), with the following thresholds: absolute $\log_2$ (fold change) > 1 and adjusted p-value < 0.05. The adjusted p-value was calculated using the Benjamini-Hochberg (BH) method to control the false discovery rate (FDR). Ferroptosis-related DEGs were then identified by intersecting this list with the previously collected FRGs.

Bioinformatics Analysis

Functional Enrichment Analysis

Gene Ontology (GO) and Kyoto Encyclopedia of Genes and Genomes (KEGG) pathway enrichment analyses were performed using the clusterProfiler package in R software. The Hs.eg.db and GOplot packages were utilized for visualization. Statistical significance was defined as an adjusted p-value < 0.05.

Protein-Protein Interaction (PPI) Network Construction

PPI networks were constructed using the STRING database (https://cn.string-db.org/). Network files in TSV format were imported into Cytoscape 3.9.1 for visualization and analysis.

Hub Gene Identification and Prognostic Analysis

Ten potential hub genes were identified using node degree and Maximum Clique Centrality (MCC) algorithms via Cytoscape's CytoHubba plugin. Prognostic significance was evaluated using Kaplan-Meier survival analysis on the GSE62452 dataset. Additional validation was performed using Xiantao Tools (https://www.xiantaozi.com/) and PanCanSurvPlot. Samples were stratified into high and low expression groups based on median gene expression levels. Log rank tests were used to assess survival differences with 95% confidence intervals.

Immune Infiltration Analysis

Immune cell infiltration patterns were analyzed using CIBERSORTx, which employs a deconvolution algorithm to quantify 22 distinct immune cell subpopulations using the LM22 signature matrix. Correlations between immune cells and hub genes were assessed using Pearson correlation analysis. Additional immune microenvironment analyses were performed using Sangerbox 3.0 (http://vip.sangerbox.com/).

Regulatory Network Construction

MicroRNA-gene and transcription factor-gene interaction networks were constructed using NetworkAnalyst (version 3.0, https://www.networkanalyst.ca/) to explore gene regulatory mechanisms. Networks were visualized using Cytoscape software.

Experimental Validation

Cell Lines and Culture Conditions

Five human pancreatic ductal adenocarcinoma (PDAC) cell lines (BxPC-3, MIA PaCa-2, PANC-1, CFPAC-1, and Capan-2) were obtained from the Cell Bank of the Chinese Academy of Sciences (Shanghai, China). BxPC-3 cells were cultured in RPMI 1640 medium (Gibco, Grand Island, NY, USA), while other cell lines were maintained in Dulbecco's Modified Eagle's Medium (DMEM; Gibco). All media were supplemented with 10% fetal bovine serum (FBS; Gibco) and 1% penicillin-streptomycin. Cells were incubated at 37°C in a humidified atmosphere with 5% CO_2.

Clinical Specimens

Tumor tissues and matched adjacent non-tumorous tissues were collected from five treatment-naïve PDAC patients at Southeast University Zhongda Hospital (Nanjing, China) between January 2023 and January 2024. All tumor specimens were independently confirmed by two board-certified pathologists. The study was conducted in accordance with the Declaration of Helsinki and approved by the institutional ethics committee.

Lentiviral Transfection and Stable Cell Line Generation

Based on our bioinformatics analysis and the difference in the prognostic value of survival analysis—*NFE2L2* (encoding NRF2), *TGFB1*, and *TP53*—were selected from the top 10 candidates for further experimental validation. Stable knockdown cell lines were generated using lentiviral vectors encoding short hairpin RNAs (shRNAs) targeting NRF2, TGFB1, and TP53, with non-targeting shRNA (sh-NC) as control. PDAC cells were seeded in 24-well plates at approximately 50% confluence and transduced with lentiviral particles in the presence of 8 μg/mL polybrene. After 48 hours, cells were selected with 2 μg/mL puromycin and maintained in medium containing 0.2 μg/mL puromycin.

Molecular and Cellular Assays

Quantitative Reverse Transcription PCR (qRT-PCR)

Total RNA was extracted using TRIzol reagent (Beyotime, Shanghai, China) and reverse-transcribed using the SweScript RT I First Strand cDNA Synthesis Kit (Servicebio, Wuhan, China). Quantitative PCR was performed using 2×SYBR Green qPCR Master Mix (Servicebio) on an Applied Biosystems 7500 system. Relative mRNA expression was

calculated using the $2^{-}\Delta\Delta Ct$ method with β-actin as the internal control. Primer sequences are provided in Supplementary Table S1.

Western Blot Analysis

Total protein was extracted using RIPA lysis buffer (Servicebio) and quantified using a BCA protein assay kit (Keygen Biotech, Nanjing, China). Equal amounts of protein (30 μg per lane) were separated by 10% SDS-PAGE and transferred to polyvinylidene fluoride (PVDF) membranes (Millipore, Bedford, MA, USA). Membranes were blocked with 5% non-fat milk and incubated overnight at 4°C with primary antibodies: anti-NRF2 (1:2000, Proteintech), anti-TGFβ1 (1:5000, Proteintech), anti-TP53 (1:5000, Proteintech), and anti-β-actin (1:5000, Abcam). After incubation with HRP-conjugated secondary antibodies (1:5000, Servicebio), protein bands were visualized using an ECL detection kit (Servicebio).

Cell Migration Assays

Wound healing assay: BxPC-3 cells were seeded in 6-well plates and grown to 90–100% confluence. Linear scratches were created using sterile 200 μL pipette tips, and wells were washed with PBS. Wound closure was monitored at 0 and 24 hours using an inverted microscope, and closure rates were quantified using ImageJ software.

Transwell migration assay: Cell migration was assessed using Transwell chambers with 8.0 μm pore size (Corning, USA). BxPC-3 cells (5×10^4) in 100 μL serum-free medium were seeded in upper chambers, with 600 μL of 10% FBS-containing medium in lower chambers as chemoattractant. After 24 hours, non-migrated cells were removed, and migrated cells were fixed with 4% paraformaldehyde, stained with 0.1% crystal violet, and counted in five random fields per membrane.

Oxidative Stress Markers

Intracellular reactive oxygen species (ROS) levels were measured using CellROX™ Deep Red Reagent (Invitrogen) and visualized by fluorescence microscopy. Cellular malondialdehyde (MDA) content was determined using a commercial MDA Detection Kit (Solarbio, Beijing, China). The ratio of reduced to oxidized glutathione (GSH/GSSG) was measured using a GSH and GSSG Assay Kit (Beyotime, Shanghai, China). All assays were performed according to manufacturers' protocols.

Statistical Analysis

All data are presented as mean ± standard deviation (SD) from at least three independent experiments. Statistical differences between two groups were analyzed using unpaired, two-tailed Student's *t*-tests. Pearson correlation analysis was used to assess variable associations. Overall survival curves were generated using the Kaplan-Meier method and compared using Log rank tests. Statistical significance was set at $p < 0.05$. All analyses were performed using R software (version 4.2.1) or GraphPad Prism 9.0.

Results

Targets of PAAD and FRGs

We obtained RNA sequencing (RNA-seq) data of PAAD patients and healthy individuals from the GEPIA database, and further identified DEGs through rigorous screening. Rigorous screening identified 9212 DEGs ($p < 0.05$). Further filtration ($|\log2\ FC| > 1$) yielded a subset of genes, whose chromosomal distribution and expression patterns were visualized using GEPIA (Figure 1A). Up-regulated and down-regulated genes are represented in red and green, respectively. Currently, 388 ferroptosis-related genes (FRGs) were extracted from the FerrDb database. Venn diagram analysis revealed 221 genes at the intersection of PAAD-associated DEGs and FRGs (Figure 1B).

Enrichment Analysis

We conducted GO and KEGG analyses on 221 candidate DEGs to clarify their key roles and associated biological pathways. As shown in Figures 2 and 3, in the biological process-related categories, DEGs were mainly enriched in cellular response to chemical sterss, response to oxidative stress and cellular response to oxidative stress. In the cellular component-related category, DEGs were mainly enriched in secondary lysosome, autolysosome, NADPH oxidase complex and apical plasma membrane. In the molecular function-related categories, DEGs are mainly enriched in antioxidant activity, ubiquitin protein ligase binding and oxidoreductase activity (acting on NADPH). In addition,

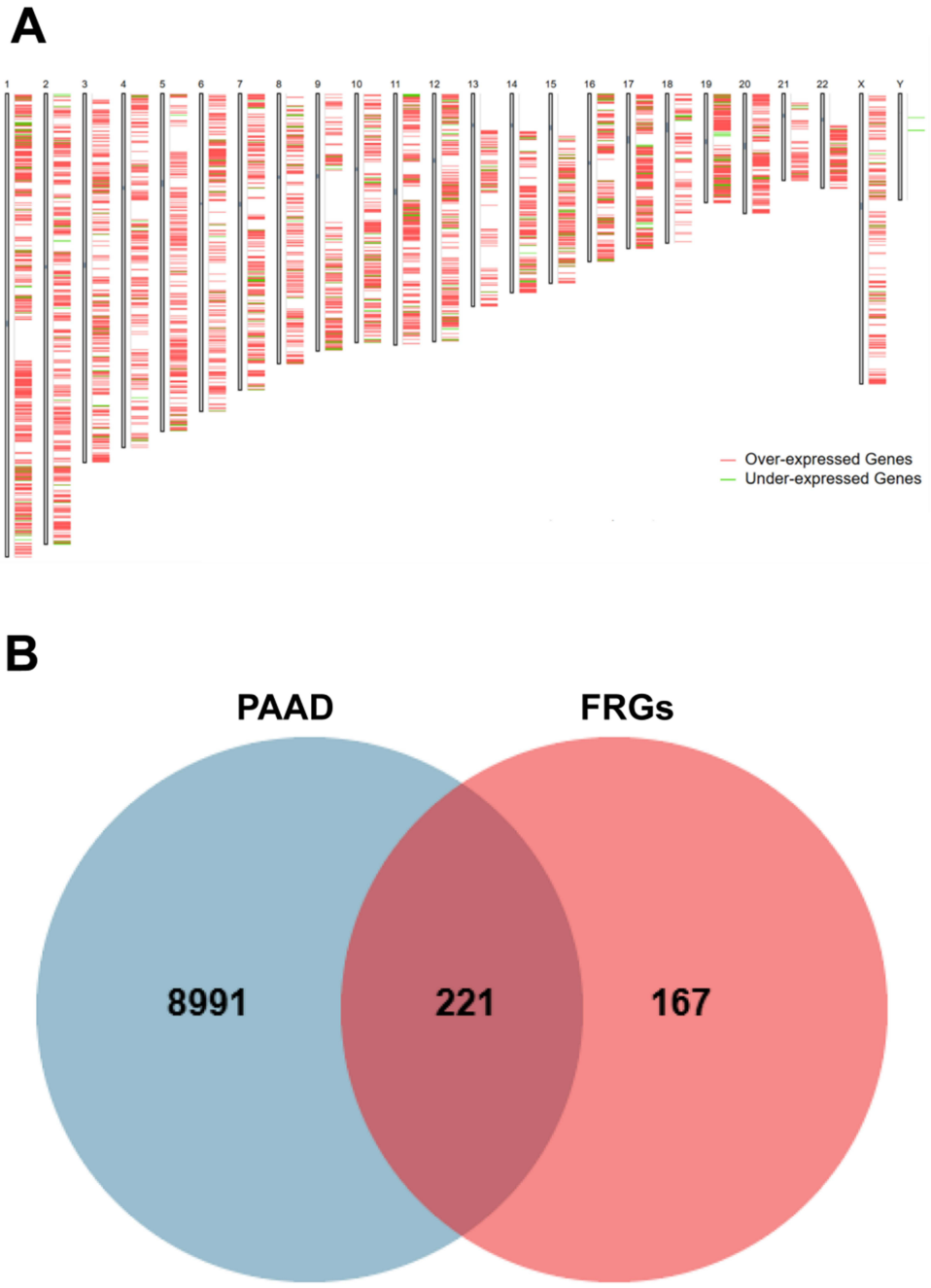

Figure 1 Analysis of gene expression in PAAD and FRGs. (**A**) Chromosomal distribution of 9212 differentially expressed genes (red: over-expressed; green: under-expressed). (**B**) Venn diagram: PAAD (8991 genes), FRGs (167 genes), and their intersection (221 DEGs).

KEGG pathway analysis showed that DEGs were mainly involved in pathways related to ferroptosis, autophagy animal and lipid and atherosclerosis pathway.

PPI Network Construction and Hub Genes Identification

Protein-protein interaction (PPI) network analysis of the overlapping differentially expressed genes (DEGs) revealed complex interconnections (Figure 4A). Further examination using the Maximal Clique Centrality (MCC) algorithm identified ten hub genes: tumor protein p53 (TP53), transforming growth factor-β1 (TGFB1), signal transducer and activator of transcription 3 (STAT3), proto-oncogene tyrosine protein kinase (SRC), prostaglandin-endoperoxide synthase

https://doi.org/10.2147/PGPM.S562602

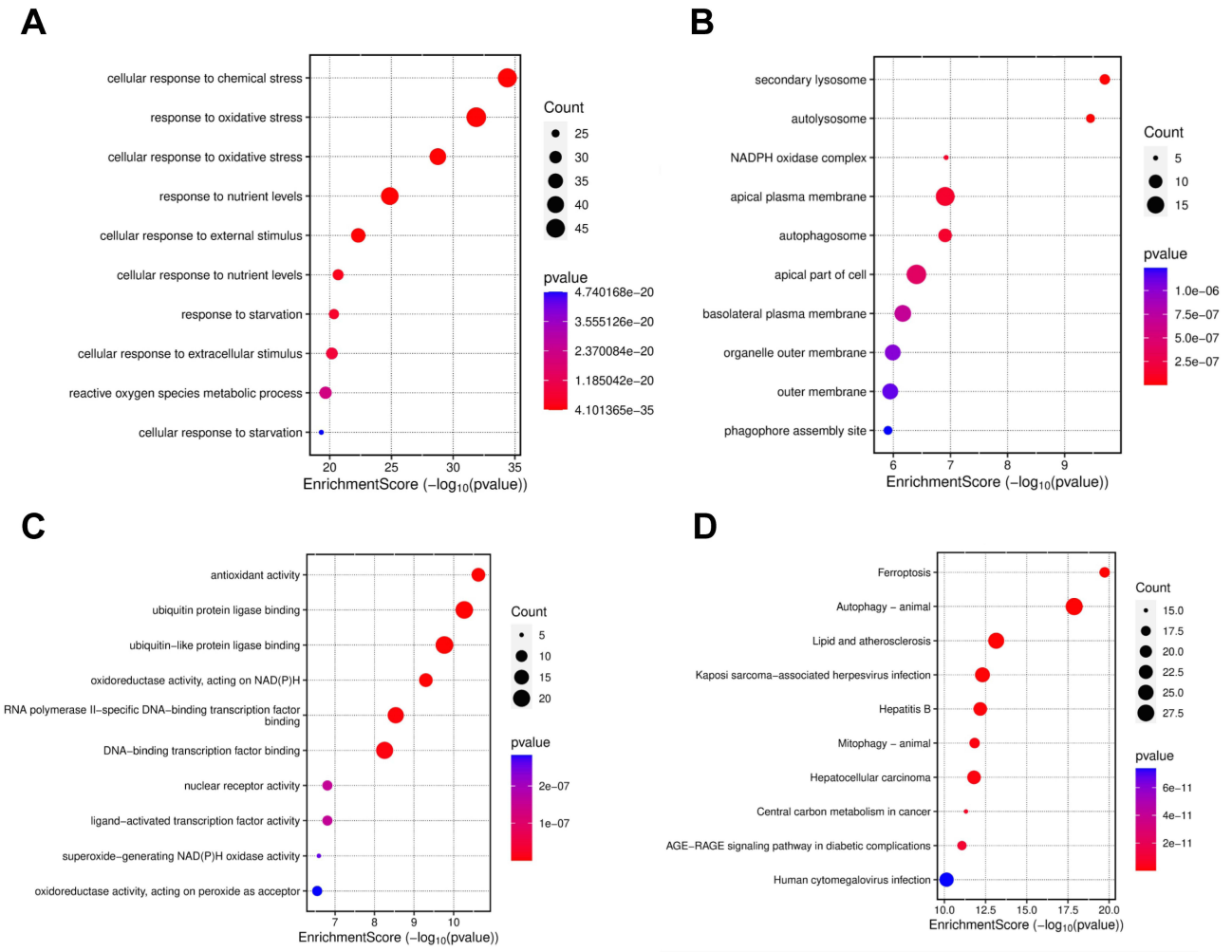

Figure 2 The GO and KEGG analysis results for 221 DEGs. (**A**) Biological process: scatter plot and table display the enrichment of DEGs in biological processes. (**B**) cellular component: scatter plot and table show the enrichment of DEGs in cellular components. (**C**) Molecular function: scatter plot and table present the enrichment of DEGs in molecular functions. (**D**) Pathway analysis: scatter plot and table illustrate the enrichment of DEGs in pathways.

2 (PTGS2), phosphatase and tensin homolog (PTEN), nuclear factor E2-related factor 2 (NFE2L2), interleukin-6 (IL6), hypoxia-inducible factor-1α (HIF1A), and albumin (ALB) (Figure 4B).

Hub Genes Survival Analysis

Whole genome sequencing data and survival data of PAAD patients were obtained from the GSE62452 dataset in the GEO database, and the 65 PAAD samples were classified into high and low expression groups according to the median expression levels of the top ten potential hub genes. The results showed that changes in the expression levels of TP53, TGFB1 and NFE2L2 were significantly correlated with the survival of PAAD patients ($p<0.05$), and high expression of TP53, TGFB1 and NFE2L2 was correlated with low survival of PAAD patients (Figure 5). In the GEPIA database, we verified that TP53, TGFB1 and NFE2L2 were highly expressed in patients (Figure 6).

Immune Cell Infiltration of Core Targets

Immune cell infiltration analysis of 65 PAAD patients revealed distinct associations between the three core genes and the tumor immune microenvironment. TP53 expression exhibited positive correlations with infiltration of activated CD4 memory T cells, activated dendritic cells, and activated mast cells, while showing negative correlations with CD8 T cells and resting CD4 memory T cells (Figure 7A). TGFB1 expression positively correlated with eosinophil infiltration and negatively correlated with activated CD4 memory T cell infiltration (Figure 7B). NFE2L2 expression demonstrated

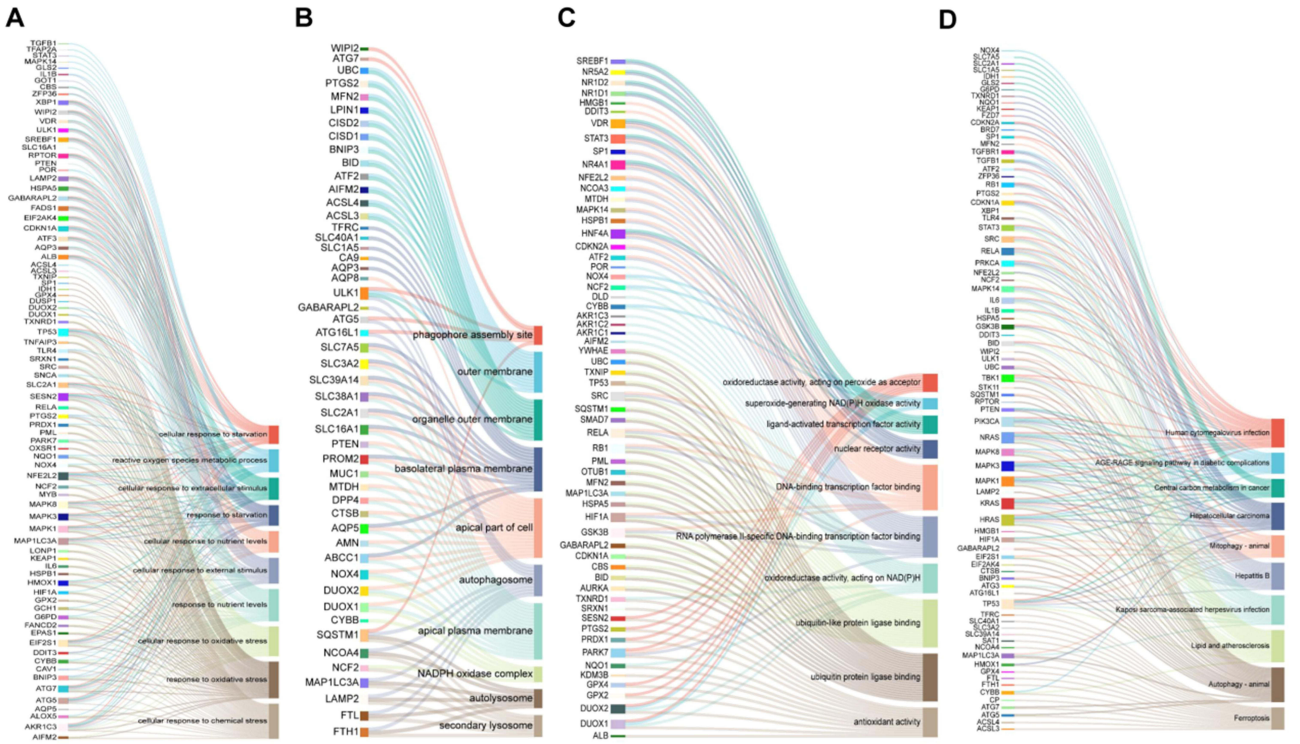

Figure 3 Sankey dot pathway enrichment. (**A**–**C**) The results of GO and (**D**) KEGG enrichment analyses for hub genes.

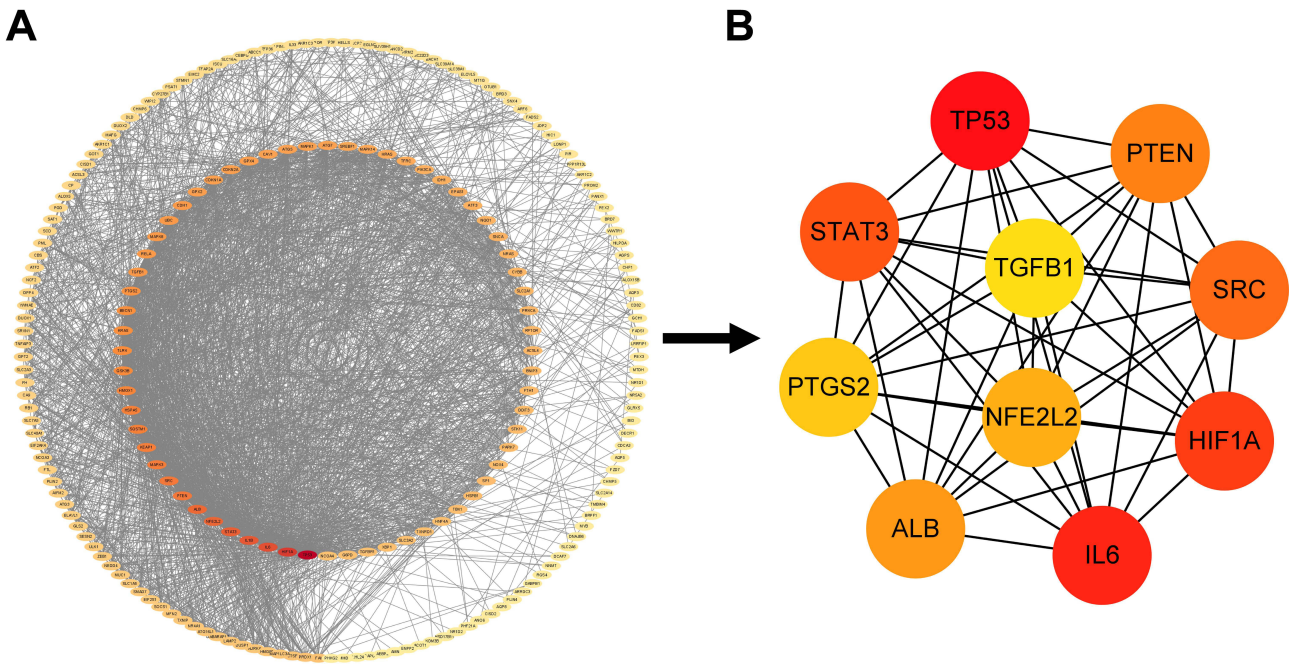

Figure 4 The Protein-protein interaction (PPI) network of 221 DEGs. (**A**) The PPI network of all 221 DEGs is depicted with nodes representing genes and edges representing interactions between them. The nodes are colored in grey, and the edges are shown in black. The outer circle contains labels of the genes. (**B**) The top 10 hub genes are identified and highlighted from the PPI network. The hub genes are represented by larger nodes in two colors: red and yellow. The red nodes indicate the most significant hub genes, while the yellow nodes represent other hub genes. The edges between the hub genes are shown in black. The labels of the top 10 hub genes are displayed next to their respective nodes.

https://doi.org/10.2147/PGPM.S562602

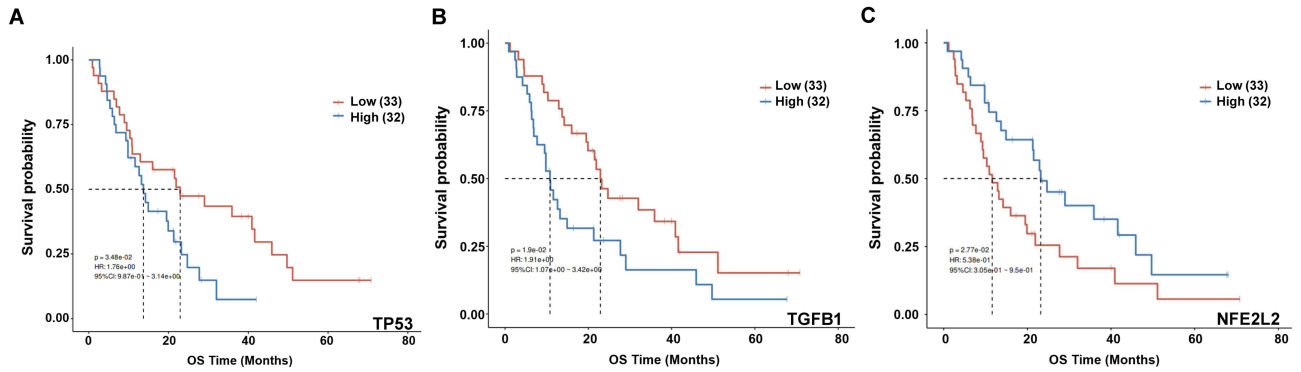

Figure 5 (**A**–**C**) OS curves for TP53, TGFB1, and NFE2L2 expression in PAAD.

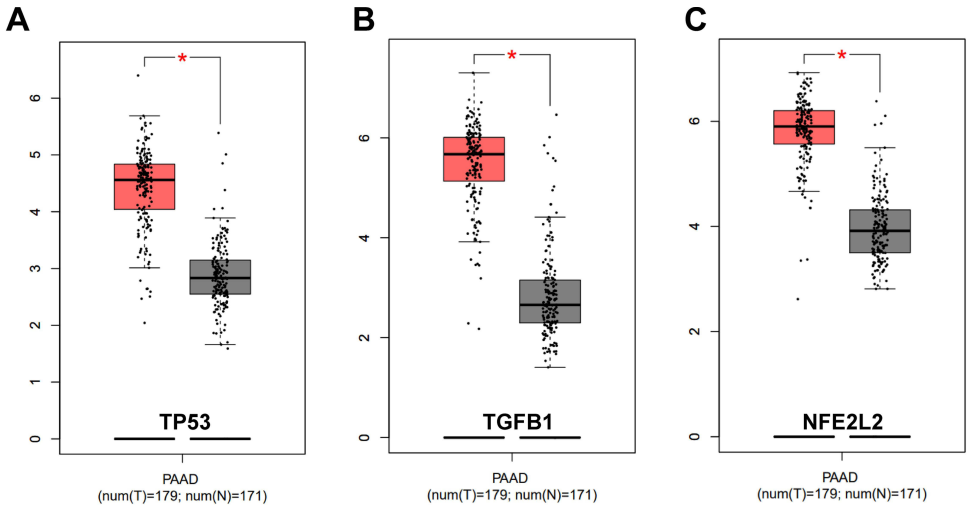

Figure 6 (**A**–**C**) 3 core genes expressed much higher in PAAD tissues than normal tissues by GEPIA, *p<0.05.

positive correlations with resting CD4 memory T cell infiltration and negative correlations with plasma cell and naive CD4 T cell infiltration (Figure 7C).

TF-Targets and miRNAs-Targets Network Construction

The Network Analyst database was employed to predict the target microRNAs (miRNAs) and transcription factors (TFs) corresponding to the core genes. miRNA-gene and TF-gene interaction networks were constructed with the assistance of Cytoscape software. The top seven target miRNAs and target TFs interacting with the core genes were identified through the use of node degree and maximum cluster centrality (MCC) algorithms, respectively. The TFs interacting with TP53, TGFB1 and NFE2L2 were JUN, CASP1, CASP3, MYC, CEBPB, EGR1 and USF1 (Figure 8A) and the miRNAs which interact with TP53, TGFB1 and NFE2L2 are hsa-mir-107, hsa-mir-34a-5p and hsa-mir-27a-3p. The remaining miRNAs were has-mir-103a-3p, has-mir-128-3p, has-mir-16-5p and has-mir-16-5p. - 16 - 5p, and has - mir - 24 - 3p (Figure 8B).

NRF2, TGFβ1, and TP53 are Upregulated in PDAC and Regulate Cell Migration and Ferroptosis

To investigate the clinical relevance of NRF2, TGFβ1, and TP53, we first examined their protein expression levels in paired tumor and adjacent non-tumorous tissues from five PDAC patients. Western blot analysis revealed that NRF2, TGFβ1, and TP53 were significantly upregulated in tumor tissues compared to their matched adjacent counterparts (Figure 9A).

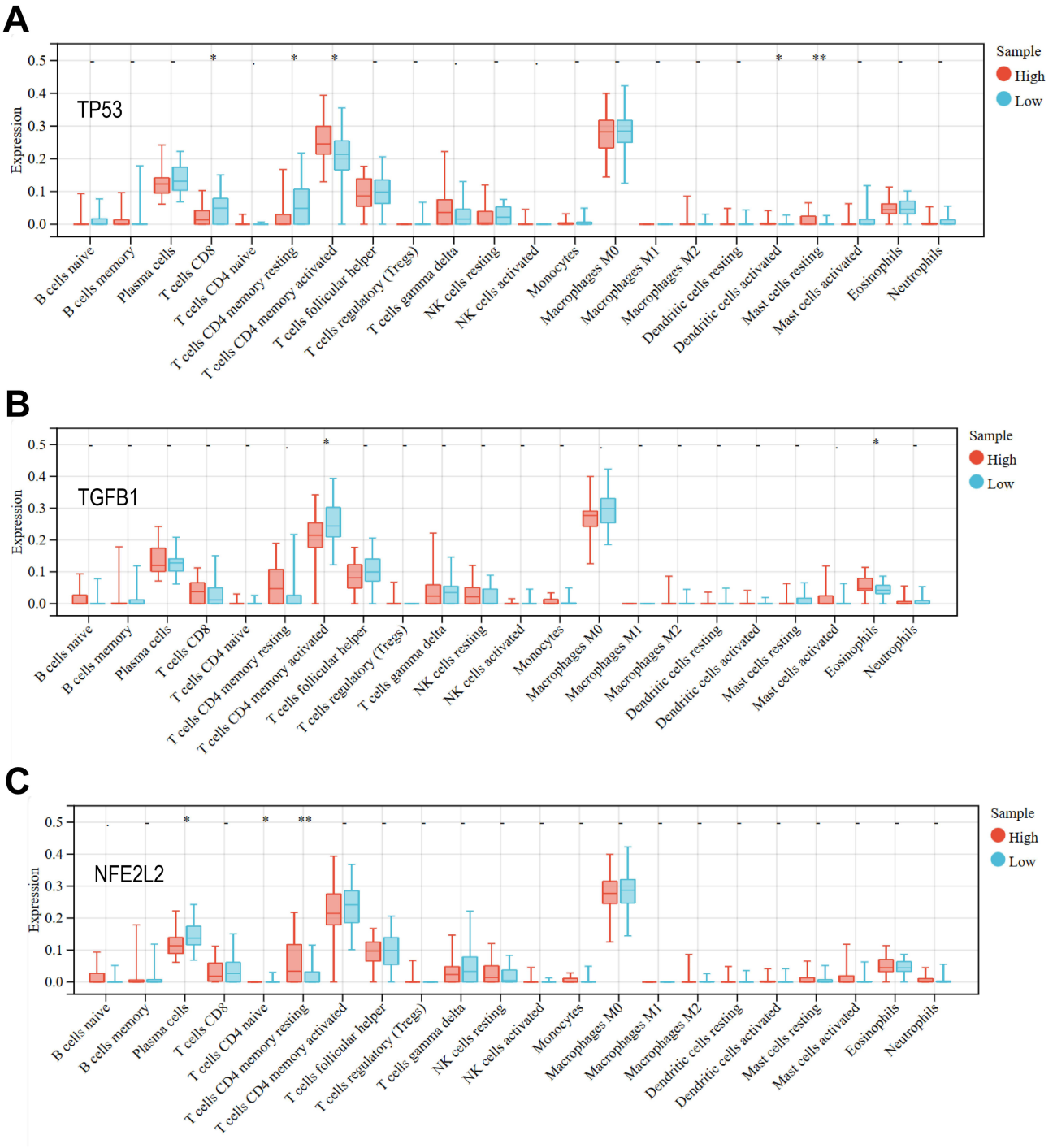

Figure 7 (**A**–**C**) Correlations of expression of four core genes (TP53, TGFB1, and NFE2L2) with immune cell infiltration.

Next, we assessed the endogenous expression of these three proteins and their corresponding mRNAs across a panel of PDAC cell lines. Consistent with the tissue data, NRF2, TGFβ1, and TP53 showed relatively high expression in MiaPaCa-2, BxPC-3, CFPAC-1, and Capan-2 cells, whereas their expression was notably lower in PANC-1 cells (Figures 9B and C). Based on its high endogenous expression levels, the BxPC-3 cell line was selected for subsequent knockdown experiments.

To elucidate the functional roles of NRF2, TGFβ1, and TP53 in PDAC progression, we established stable knockdown BxPC-3 cell lines using shRNAs. The knockdown efficiency was confirmed at both the mRNA and protein levels

https://doi.org/10.2147/PGPM.S562602

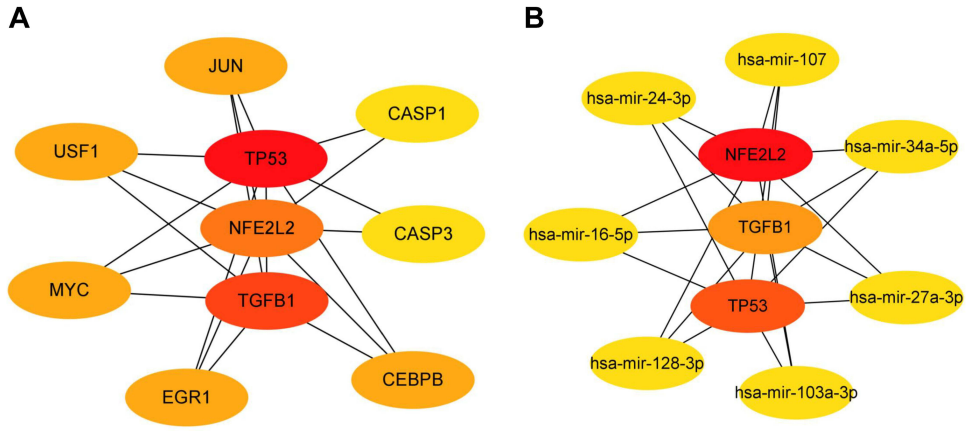

Figure 8 (**A**) TF-Targets and (**B**) miRNAs-Targets network construction.
Abbreviation: miRNA, microRNA.

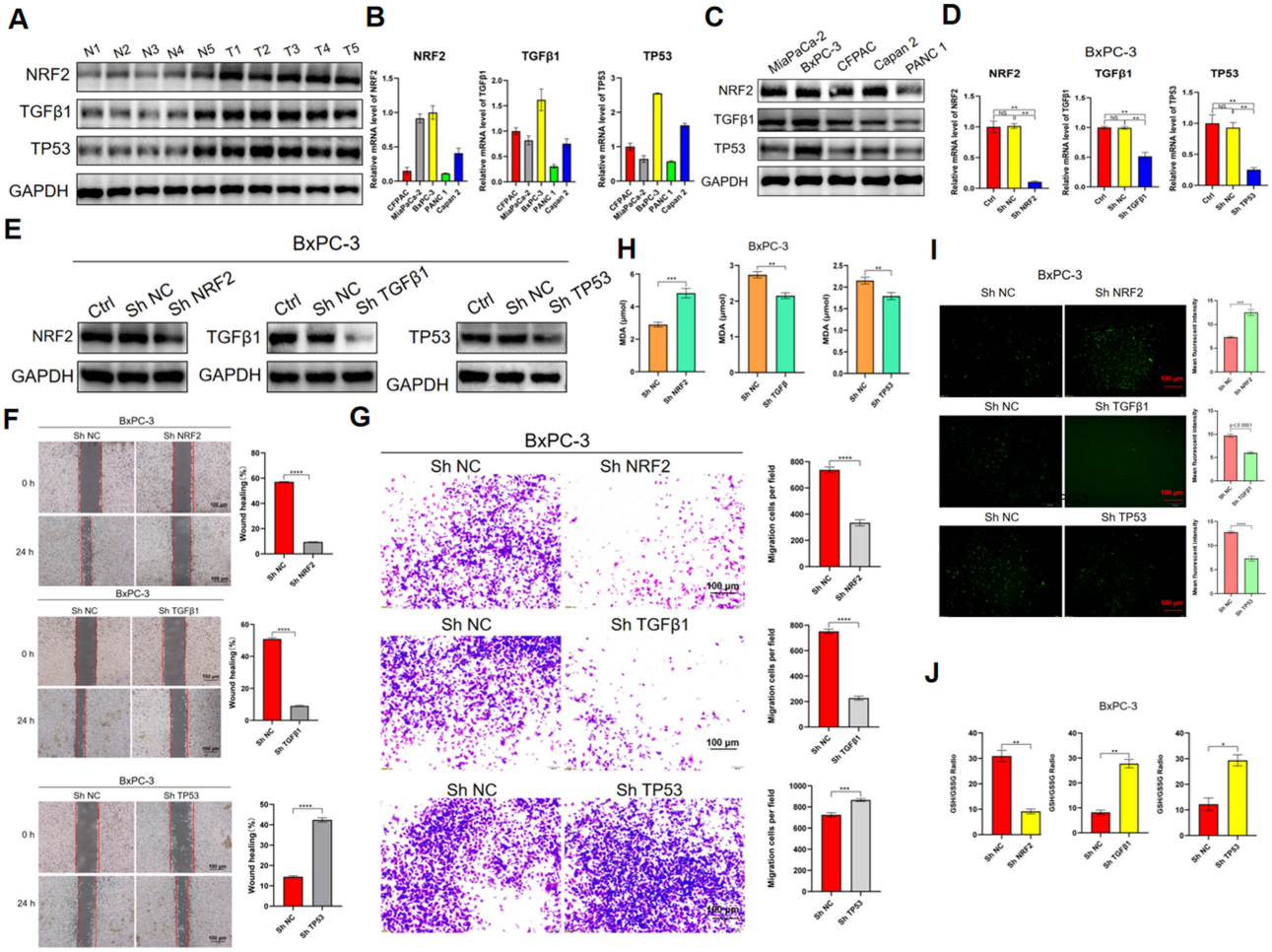

Figure 9 (**A**) Expression levels of NRF2, TGFβ1, and TP53 in tumor tissues versus adjacent tissues as determined by Western blot analysis. (**B** and **C**) mRNA and protein expression levels of NRF2, TGFβ1, and TP53 in various PDAC cell lines. (**D** and **E**) Knockdown efficiency of NRF2, TGFβ1, and TP53 in BxPC-3 cells. (**F**) Wound healing assay demonstrating the effects of NRF2, TGFβ1and TP53 knockdown on cell migration in BxPC-3 cells. (**G**) Transwell assay results illustrating the migration capability of MiaPaCa-2 cells following knockdown of NRF2, TGFβ1, and TP53. (**H-J**) Levels of MDA, ROS, and GSH/GSSG in BxPC-3 cells with knockdown of NRF2, TGFβ1, and TP53, indicating their effects on ferroptosis.

https://doi.org/10.2147/PGPM.S562602

(Figures 9D and E). We then evaluated the impact of gene silencing on cell migration using wound healing and Transwell assays. The wound healing assay demonstrated that compared to the non-targeting control (sh-NC) group, knockdown of NRF2 or TGFB1 significantly impaired wound closure by 501.67% and 465.78% respectively ($p<0.0001$). Conversely, knockdown of TP53 markedly accelerated wound closure by 193.36% ($p<0.0001$)(Figure 9F). These findings were corroborated by the Transwell migration assay, which showed that silencing NRF2 or TGFB1 inhibited BxPC-3 cell migration by 120.86% and 230.65% respectively ($p<0.0001$), while silencing TP53 enhanced it by 19.36% ($p=0.0004$) (Figure 9G).

Given the established connection of these genes to ferroptosis, we further investigated their role in regulating this process in PDAC cells by measuring key ferroptosis markers. Knockdown of NRF2 in BxPC-3 cells significantly increased malondialdehyde (MDA) by 66.83% ($p=0.0005$) and increased reactive oxygen species (ROS) levels by 70.56% ($P=0.0002$), along with decreased in the GSH/GSSG ratio by 237.76% ($p=0.0021$). In contrast, knockdown of TGFB1 led to decreased MDA by 28.18% ($p=0.0010$), decreased ROS levels by 61.06% ($p<0.0001$) and increased GSH/GSSG ratio by 237.55% ($p=0.0031$). Knockdown of TP53 led to decreased MDA by 20.09% ($p=0.0053$), decreased ROS levels by 75.03% ($p<0.0001$) and increased GSH/GSSG ratio by 268.34% ($p=0.0237$) (Figure 9H–J).

Discussion

Pancreatic cancer, one of the most aggressive malignancies, has seen a doubling in global annual diagnoses over the past two decades. Despite this high incidence rate, survival rates remain dismally low.[30] Although the overall five-year survival rate has shown some improvement, increasing from less than 5% in the 1990s to approximately 9% in the United States and Europe as of 2019, it still remains one of the lowest among all cancer types.[31,32] In recent years, the targeting of alternative cell death pathways, such as ferroptosis, has emerged as a promising therapeutic strategy. This is due to the fact that PAAD cells exhibit inherent metabolic vulnerabilities, including abnormal iron metabolism and heightened oxidative stress sensitivity. These vulnerabilities render the cells susceptible to ferroptotic induction. However, the key regulators orchestrating ferroptosis in PAAD and their functional crosstalk with tumor progression and the immune microenvironment remain incompletely defined. This study integrates bioinformatic analysis and in vitro validation to identify TP53, TGFB1, and NFE2L2 (encoding NRF2) as ferroptosis-related hub genes in PAAD, and systematically characterises their differential roles in modulating cell migration and ferroptosis sensitivity, providing novel insights into the molecular mechanisms underlying PAAD pathogenesis.

Bioinformatics analysis identified 221 ferroptosis-related differentially expressed genes in PAAD. These genes were found to be significantly enriched in various biological processes, including the cellular response to oxidative stress and antioxidant activity, as well as signaling pathways such as ferroptosis and autophagy. These findings are consistent with the well-recognized view that oxidative stress dysregulation is a hallmark of the development of PAAD.[33,34] The enrichment of differentially expressed genes in the NADPH oxidase complex and oxidoreductase activity highlights the crucial role of reactive oxygen species (ROS) metabolism in the progression of pancreatic cancer. Elevated ROS levels have been demonstrated to drive lipid peroxidation (a core event in ferroptosis) and to activate pro-survival and pro-metastatic signaling pathways, consequently resulting in treatment resistance.[35,36] Furthermore, the enrichment of differentially expressed genes in biological processes such as ubiquitin-protein ligase binding and antioxidant activity suggests that post-translational regulatory mechanisms may fine-tune the sensitivity of pancreatic cancer cells to ferroptosis, a hypothesis which merits further investigation. The results of these enrichment analyses indicate widespread dysregulation of ferroptosis-related signaling pathways in pancreatic cancer, thus supporting the concept that these pathways could be targeted for therapeutic intervention.

The protein-protein interaction network analysis identified ten hub genes, with TP53, TGFB1, and NFE2L2 emerging as the most significant based on survival analysis. Our experimental validation confirmed that TP53, TGFB1, and NFE2L2 are highly expressed in PAAD tissues, supporting our bioinformatics findings. The role of TP53 in PAAD is characterised by complex allele- and environment-specificity. In the present study, high expression of TP53 was found to be associated with poor patient survival, a pattern typically driven by the accumulation of gain-of-function (GOF) mutant p53 proteins in tumors.[37] In BxPC-3 cell experiments, TP53 knockdown significantly enhanced cell migration ability while reducing ferroptosis, indicating that p53 still retains tumor-suppressive activity in this cellular environment,

promoting cell sensitivity to ferroptosis and inhibiting cell motility. This observation, which at first glance appears contradictory, is rooted in the finding that tumors exhibiting GOF p53 mutants may manifest oncogenic characteristics, thereby concealing some of the cell-autonomous tumor-suppressive functions observed in in vitro experiments.

In contrast to TP53, the function of NFE2L2 is entirely consistent with its established role as a core regulator of cancer malignancy, possessing both pro-migratory and anti-ferroptotic functions. This phenomenon is contingent upon a dual mechanism that is facilitated by NRF2. On the one hand, it coordinates metabolic reprogramming towards the pentose phosphate pathway, thereby providing the reduced coenzyme II (NADPH) that is required for the elevated biosynthetic and redox demands of migrating cells.[38] Conversely, it has been observed that the formation of a "redox barrier" contributes to the tolerance of invasive cells towards the intrinsic oxidative stress associated with motility and matrix detachment. The research found that as the main regulator of antioxidant defense, the degradation of NRF2 can significantly increase the level of reactive oxygen species (ROS) and the accumulation of malondialdehyde (MDA), which may effectively eliminate the intrinsic resistance of cancer cells to ferroptosis.[39,40] In contrast, TP53 has been demonstrated to act as a driver of ferroptosis, possibly through the process of transcriptional repression of SLC7A11. This hypothesis has been widely supported in the extant literature.[41,42] The antagonistic relationship between NRF2 and TP53 observed in network analysis highlights a key survival strategy of PAAD cells: tumor cells may upregulate NRF2 to counteract the metabolic stress and potential ferroptosis induced by oncogenic signals or TP53 activity.

Perhaps the most intriguing finding is the dual functionality of TGFB1, which our data show promotes both cell migration and ferroptosis sensitivity. This apparent paradox can be reconciled by viewing these functions not as contradictory, but as components of a sophisticated biological strategy that ultimately benefits tumor fitness. This seemingly contradictory phenomenon is consistent with the concept of "ferroptosis addiction". The pro-migratory capacity of TGFB1 is a well-documented hallmark of its late-stage, pro-tumorigenic role, driven by the canonical activation of the epithelial-mesenchymal transition (EMT) program[43]. Our data robustly confirm this function in PAAD cells. Concurrently, the pro-ferroptotic action of TGFB1 is explained by recent mechanistic discoveries demonstrating that TGF-β signaling, via SMAD3, can directly repress the transcription of SLC7A11 (xCT), a key anti-ferroptosis gene, thereby depleting glutathione and sensitizing cells to lipid peroxidation.[44] We propose a model of spatiotemporal compartmentalization to resolve this duality: at the well-nourished invasive front, the pro-EMT effects of TGFB1 dominate, whereas in the hypoxic and nutrient-deprived tumor core, its pro-ferroptotic pressure prevails, potentially acting as a "metabolic pruning" mechanism. This process does not represent a net tumor-suppressive effect; rather, it imposes a strong selective pressure, favoring the survival and dissemination of clones that have acquired robust ferroptosis resistance mechanisms, such as NRF2 hyperactivation. This evolutionary dynamic explains why high TGFB1 expression, despite its pro-ferroptotic liability, is ultimately correlated with a more aggressive phenotype and poorer patient survival. The dual role of TGFB1, in conjunction with the regulatory interaction of the TP53/TGFB1/NRF2 axis, engenders a unique therapeutic window. It has been established that highly metastatic tumors driven by TGFB1, despite their significant malignant phenotypes, have an intrinsic sensitivity to ferroptosis inducers due to a phenomenon of "ferroptosis addiction". Consequently, as long as the antioxidant buffering capacity mediated by NRF2 (which can counteract ferroptosis stress) is simultaneously blocked, ferroptosis inducers can be used to effectively target these malignant tumors.

The immune infiltration analysis revealed distinct correlations between core gene expression and immune populations, consistent with ferroptosis's role in immune regulation.[45] For instance, TP53 positively correlated with activated CD4 memory T cells and dendritic cells, potentially influencing immune surveillance.[22,46] TGFB1 correlated with eosinophil infiltration, which may promote tumorigenesis via mediators.[47,48] NFE2L2 showed correlations with resting CD4 memory T cells, possibly modulating redox-dependent immune functions.[49] These suggest a complex immunoregulatory loop in PAAD,[50,51] though limited by lack of experimental validation or patient-level correlations; future studies should incorporate immunohistochemistry or single-cell analyses for confirmation.

The identification of key miRNAs and TFs interacting with the core genes provides insight into the regulatory networks governing ferroptosis in PAAD. miRNAs such as hsa-mir-34a-5p and hsa-mir-27a-3p have been previously implicated in cancer progression and therapy resistance[52,53] The involvement of these miRNAs in regulating ferroptosis-related genes suggests potential therapeutic opportunities through miRNA modulation. Similarly, the identified TFs, including JUN and MYC, are known to play crucial roles in oncogenesis and may modulate ferroptosis sensitivity in

PAAD.[54] These findings collectively suggest a complex interplay between ferroptosis-related genes, immune regulation, and PAAD progression.

Consequently, this study proposes a relevant scientific hypothesis. In the context of PAAD, the TP53/TGFB1/NRF2 axis exerts its regulatory influence over ferroptosis sensitivity through a dual modality comprising functional antagonism and spatiotemporal synergy. Concurrently, it has been observed that this process is associated with the migration of tumor cells and the remodeling of the immune microenvironment, ultimately resulting in the malignant transformation of tumors. The evidence suggests that TP53 and TGFB1 jointly promote ferroptosis, while NRF2 reversely inhibits ferroptosis, and the three form a dynamic balance between pro-ferroptosis and anti-ferroptosis. When the balance shifts towards NRF2 (excessive activation of NRF2), tumor cells develop ferroptosis resistance and high migration ability, manifesting as a malignant phenotype. In circumstances where the balance is found to be tipped in favour of TP53/TGFB1 (blocking NRF2), it has been demonstrated that the ferroptosis sensitivity of tumor cells is increased and their migration ability is inhibited[28,44,55–58] (Supplementary Figure S1). This provides a theoretical basis for the development of effective treatment strategies.

The translation of these molecular research findings into clinical practice is contingent upon precise patient stratification. Patients exhibiting the characteristic features of NRF2 (high)/TP53 (mut/low) may possess a robust antioxidant defence capacity and demonstrate resistance to conventional chemotherapy or single-agent ferroptosis inducers. For this subgroup of patients, a combination therapy strategy is proposed, involving the initial use of pharmacological NRF2 inhibitors (brusatol or its clinical derivatives) to lower the ferroptosis threshold, followed by the administration of ferroptosis inducers (erastin or sorafenib) for treatment. The correlation between epithelial-mesenchymal transition (EMT) and ferroptosis susceptibility suggests that patients with the TGFB1 (high) type may exhibit a favourable response to drugs targeting the lipid peroxidation pathway, thereby converting their metastasis drivers into metabolic vulnerabilities. In the future, precision oncology trials for pancreatic cancer may wish to consider evaluating this genetic signature as a means of predicting treatment response.

Whilst the present findings offer a promising mechanistic framework, it is important to acknowledge several limitations. Firstly, it is important to note that the conclusions regarding the therapeutic efficacy of the drug in question are primarily based on bioinformatic predictions and in vitro experiments using the BxPC-3 cell line. The complex tumor microenvironment (TME) has a profound impact on TGFB1 signaling and immune infiltration, and the existing experimental conditions may not fully reproduce the microenvironment in the bodies of PAAD patients. Secondly, the clinical sample size employed for validation purposes was relatively modest, a factor that necessitates a cautious approach when generalising the potential of this axis as a biomarker. Thirdly, this study did not involve the performance of in vivo experiments. It is vital that future investigations utilise patient-derived xenografts (PDX) or genetically engineered mouse models (GEMM) in order to confirm whether targeting the TP53/TGFB1/NRF2 axis can effectively reduce tumor size and prevent metastasis in a living organism. Consequently, the therapeutic strategies proposed here should be regarded as preliminary hypotheses that require rigorous preclinical evaluation.

Conclusion

In summary, this study integrates bioinformatic analysis with in vitro validation to identify TP53, TGFB1, and NFE2L2 (NRF2) as a critical regulatory axis orchestrating the balance between ferroptosis sensitivity and metastatic potential in PAAD. The data presented herein reveal distinct and partially antagonistic roles within this triad: NRF2 functions as a primary resistance factor, promoting migration while suppressing ferroptosis; TGFB1 exhibits a dual role by driving migration yet sensitising cells to ferroptosis; and TP53 acts to restrain migration while promoting ferroptotic cell death. These findings suggest that the TP53/TGFB1/NRF2 signature could serve as a potential biomarker for patient stratification. For instance, patients exhibiting an NRF2 (high)/TP53 (mut/low) profile may benefit from combinatorial therapies that employ ferroptosis inducers in conjunction with NRF2 inhibitors to circumvent intrinsic resistance. However, it must be acknowledged that these conclusions are merely preliminary, as they are primarily based on bioinformatic predictions and functional validation in the BxPC-3 cell line. The present study is constrained by two factors: firstly, the clinical sample size is limited; and secondly, the absence of in vivo animal models. It is imperative that future investigations

utilise diverse genetic backgrounds and patient-derived xenografts (PDX) in order to fully validate the therapeutic viability of targeting this axis in a clinical setting.

Data Sharing Statement

The datasets generated and/or analysed during the current study are not publicly available due confidentiality concerns related to the proprietary nature of the data but are available from the corresponding author Xu tonglei on reasonable request.

Ethics Approval and consent to participate

This study was approved by the Ethics Committee of Southeast University Zhongda Hospital (Ethical No.: 2024ZDSYLL378-P01). All patients provided written informed consent to participate in the study.

Acknowledgments

We would like to thank the Xu tonglei from the Southeast University for his help and technical support.

Funding

This project was funded by Lianyungang Anti Cancer Association Cancer Prevention and Treatment Technology Development Plan Project (No.: MS202301).

Disclosure

The author(s) report no conflicts of interest in this work.

References

1. Siegel RL, Miller KD, Fuchs HE, et al. Cancer statistics, 2022. *CA Cancer J Clin*. 2022;72(1):7–33. doi:10.3322/caac.21708
2. Rahib L, Smith BD, Aizenberg R, et al. Projecting cancer incidence and deaths to 2030: the unexpected burden of thyroid, liver, and pancreas cancers in the United States. *Cancer Res*. 2014;74(11):2913–2921. doi:10.1158/0008-5472.CAN-14-0155
3. Zhang L, Sanagapalli S, Stoita A. Challenges in diagnosis of pancreatic cancer. *World J Gastroenterol*. 2018;24(19):2047–2060. doi:10.3748/wjg.v24.i19.2047
4. Kommalapati A, Tella SH, Goyal G, et al. Contemporary management of localized resectable pancreatic cancer. *Cancers*. 2018;10(1):24. doi:10.3390/cancers10010024
5. Siegel RL, Miller KD, Fuchs HE, et al. Cancer statistics, 2021. *CA Cancer J Clin*. 2021;71(1):7–33. doi:10.3322/caac.21654
6. Canto MI, Harinck F, Hruban RH, et al. International Cancer of the Pancreas Screening (CAPS) consortium summit on the management of patients with increased risk for familial pancreatic cancer. *Gut*. 2013;62:339–347. doi:10.1136/gutjnl-2012-303108
7. World Health Organization. Cancer prevention and control in the context of an integrated approach: report by the secretariat. 2016.
8. Poruk KE, Firpo MA, Adler DG, et al. Screening for pancreatic cancer: why, how, and who? *Ann Surg*. 2013;257:17–26. doi:10.1097/SLA.0b013e31825ffbfb
9. Neoptolemos JP, Kleeff J, Michl P, et al. Therapeutic developments in pancreatic cancer: current and future perspectives. *Nat Rev Gastroenterol Hepatol*. 2018;15:333–348. doi:10.1038/s41575-018-0005-x
10. Keane MG, Horsfall L, Rait G, et al. A case-control study comparing the incidence of early symptoms in pancreatic and biliary tract cancer. *BMJ Open*. 2014;4:e005720. doi:10.1136/bmjopen-2014-005720
11. Zhou Y, Abel GA, Hamilton W, et al. Diagnosis of cancer as an emergency: a critical review of current evidence. *Nat Rev Clin Oncol*. 2017;14:45–56. doi:10.1038/nrclinonc.2016.155
12. Hippisley-Cox J, Coupland C. Identifying patients with suspected pancreatic cancer in primary care: derivation and validation of an algorithm. *Br J Gen Pract*. 2012;62:e38–45. doi:10.3399/bjgp12X616355
13. Stapley S, Peters TJ, Neal RD, et al. The risk of pancreatic cancer in symptomatic patients in primary care: a large case-control study using electronic records. *Br J Cancer*. 2012;106:1940–1944. doi:10.1038/bjc.2012.190
14. Kamisawa T, Wood LD, Itoi T, et al. Pancreatic cancer. *Lancet*. 2016;388:73–85. doi:10.1016/S0140-6736(16)00141-0
15. Pereira SP, Oldfield L, Ney A, et al. Early detection of pancreatic cancer. *Lancet Gastroenterol Hepatol*. 2020;5(7):698–710. doi:10.1016/S2468-1253(19)30416-9
16. Zeng S, Pöttler M, Lan B, et al. Chemoresistance in pancreatic cancer. *Int J Mol Sci*. 2019;20(18):4504. doi:10.3390/ijms20184504
17. Bailey P, Chang DK, Nones K, et al. Genomic analyses identify molecular subtypes of pancreatic cancer. *Nature*. 2016;531(7592):47–52.
18. Buscail L, Bournet B, Cordelier P. Role of oncogenic KRAS in the diagnosis, prognosis and treatment of pancreatic cancer. *Nat Rev Gastroenterol Hepatol*. 2020;17(3):153–168. doi:10.1038/s41575-019-0245-4
19. Tang B, Li Y, Qi G, et al. Clinicopathological significance of CDKN2A promoter hypermethylation frequency with pancreatic cancer. *Sci Rep*. 2015;5:13563. doi:10.1038/srep13563
20. Sun S, Shen J, Jiang J, et al. Targeting ferroptosis opens new avenues for the development of novel therapeutics. *Signal Transduct Target Ther*. 2023;8(1):372. doi:10.1038/s41392-023-01606-1

21. Dixon SJ, Lemberg KM, Lamprecht MR, et al. Ferroptosis: an iron-dependent form of nonapoptotic cell death. *Cell*. 2012;149(5):1060–1072. doi:10.1016/j.cell.2012.03.042
22. Friedmann Angeli JP, Krysko DV, Conrad M, et al. Ferroptosis at the crossroads of cancer-acquired drug resistance and immune evasion. *Nat Rev Cancer*. 2019;19(7):405–414. doi:10.1038/s41568-019-0149-1
23. De Santis MC, Bockorny B, Hirsch E, et al. Exploiting pancreatic cancer metabolism: challenges and opportunities. *Trends Mol Med*. 2024;30(6):592–604. doi:10.1016/j.molmed.2024.03.008
24. Jiang X, Stockwell BR, Conrad M. Ferroptosis: mechanisms, biology and role in disease. *Nat Rev Mol Cell Biol*. 2021;22(4):266–282. doi:10.1038/s41580-020-00324-8
25. Lei G, Zhuang L, Gan B. Targeting ferroptosis as a vulnerability in cancer. *Nat Rev Cancer*. 2022;22(7):381–396. doi:10.1038/s41568-022-00459-0
26. Zhang Y, Yu R, Li Q, et al. Epigenetic suppression of Nrf2-Slc40a1 axis induces ferroptosis and enhances immunotherapy in pancreatic cancer. *J Immunother Cancer*. 2025;13(10): e013269. doi:10.1136/jitc-2025-013269
27. Yuan Y, Zhai Y, Chen J, Xu X, Wang H. Kaempferol ameliorates oxygen-glucose deprivation/reoxygenation-induced neuronal ferroptosis by activating Nrf2/SLC7A11/GPX4 axis. *Biomolecules*. 2021;11(7):923. doi:10.3390/biom11070923
28. Kang R, Kroemer G, Tang D. The tumor suppressor protein p53 and the ferroptosis network. *Free Radic Biol Med*. 2019;133:162–168. doi:10.1016/j.freeradbiomed.2018.05.074
29. Yang D, Wang X, Sun Y, Shao Y, Shi X. Identification and experimental validation of genes associated with programmed cell death in dendritic cells of the thyroid tissue in Hashimoto's thyroiditis. *Int Immunopharmacol*. 2024;142(Pt A):113083. doi:10.1016/j.intimp.2024.113083
30. P KA. Pancreatic cancer epidemiology: understanding the role of lifestyle and inherited risk factors. *Nat Rev Gastroenterol Hepato*. 2021;18(7):493–502. doi:10.1038/s41575-021-00457-x
31. Siegel RL, Miller KD, Jemal A. Cancer statistics, 2020. *CA Cancer J Clin*. 2020;70(1):7–30. doi:10.3322/caac.21590
32. Stockwell BR, Angeli JP, Bayir H, et al. Ferroptosis: a regulated cell death nexus linking metabolism, redox biology, and disease. *Cell*. 2017;171(2):273–285. doi:10.1016/j.cell.2017.09.021
33. Hayes JD, Dinkova-Kostova AT, Tew KD. Oxidative stress in cancer. *Cancer Cell*. 2020;38:167–197. doi:10.1016/j.ccell.2020.06.001
34. Li K, Deng Z, Lei C, Ding X, Li J, Wang C. The role of oxidative stress in tumorigenesis and progression. *Cells*. 2024;13:441. doi:10.3390/cells13050441
35. Nakamura H, Takada K. Reactive oxygen species in cancer: current findings and future directions. *Cancer Sci*. 2021;112:3945–3952. doi:10.1111/cas.15068
36. Luo M, Zhou L, Huang Z, et al. Antioxidant therapy in cancer: rationale and progress. *Antioxidants*. 2022;11:1128. doi:10.3390/antiox11061128
37. Muller PA, Vousden KH. Mutant p53 in cancer: new functions and therapeutic opportunities. *Cancer Cell*. 2024;25(3):304–317.
38. DeNicola GM, Chen PH, Mullarky E, et al. NRF2 regulates serine biosynthesis in non-small cell lung cancer. *Nat Genet*. 2015;47(12):1475–1481. doi:10.1038/ng.3421
39. Wu Y, Pi D, Zhou S, et al. Ginsenoside Rh3 induces pyroptosis and ferroptosis through the Stat3/p53/NRF2 axis in colorectal cancer cells. *Acta Biochim Biophys Sin*. 2023;55(4):587–600. doi:10.3724/abbs.2023068
40. Liu JZ, Hu YL, Feng Y, et al. BDH2 triggers ROS-induced cell death and autophagy by promoting Nrf2 ubiquitination in gastric cancer. *J Exp Clin Cancer Res*. 2020;39(1):123. doi:10.1186/s13046-020-01620-z
41. Zhao H, Li X, Yang L, et al. Isorhynchophylline relieves ferroptosis-induced nerve damage after intracerebral hemorrhage via miR-122-5p/TP53/SLC7A11 pathway. *Neurochem Res*. 2021;46(8):1981–1994. doi:10.1007/s11064-021-03320-2
42. Xin Z, Hu C, Zhang C, et al. LncRNA-HMG incites colorectal cancer cells to chemoresistance via repressing p53-mediated ferroptosis. *Redox Biol*. 2024;77:103362. doi:10.1016/j.redox.2024.103362
43. Lamouille S, Xu J, Derynck R. Molecular mechanisms of epithelial-mesenchymal transition. *Nat Rev Mol Cell Biol*. 2014;15(3):178–196. doi:10.1038/nrm3758
44. Kim DH, Kim WD, Kim SK, et al. TGF-β1-mediated repression of SLC7A11 drives vulnerability to GPX4 inhibition in hepatocellular carcinoma cells. *Cell Death Dis*. 2020;11(5):406. doi:10.1038/s41419-020-2618-6
45. Dodson M, Castro-Portuguez R, Zhang DD. NRF2 plays a critical role in mitigating lipid peroxidation and ferroptosis. *Redox Biol*. 2019;23:101107. doi:10.1016/j.redox.2019.101107
46. de la Vega M R, Chapman E, Zhang DD, et al. NRF2 and the hallmarks of cancer. *Cancer Cell*. 2018;34(1):21–43. doi:10.1016/j.ccell.2018.03.022
47. L L-TG, N AE, A MD, et al. Immunometabolism of ferroptosis in the tumor microenvironment. *Front Oncol*. 2024;14:1441338. doi:10.3389/fonc.2024.1441338
48. Grisaru-Tal S, Itan M, Klion AD, et al. A new dawn for eosinophils in the tumor microenvironment. *Nat Rev Cancer*. 2020;20(10):594–607. doi:10.1038/s41568-020-0283-9
49. Manohar M, Verma AK, Venkateshaiah SU, et al. Significance of eosinophils in promoting pancreatic malignancy. *J Gastroenterol Pancreatol Liver Disord*. 2017;5(1). doi:10.15226/2374-815X/5/1/001109
50. Haque S, Morris JC. Transforming growth factor-β: a therapeutic target for cancer. *Hum Vaccin Immunother*. 2017;13(8):1741–1750. doi:10.1080/21645515.2017.1327107
51. Feng B, Wu J, Shen B, et al. Cancer-associated fibroblasts and resistance to anticancer therapies: status, mechanisms, and countermeasures. *Cancer Cell Int*. 2022;22(1):166. doi:10.1186/s12935-022-02599-7
52. Noorolyai S, Baghbani E, Rahmani S, et al. hsa-miR-34a-5p potentiates cytarabine-mediated cell cycle arrest in MDA-MB-231 cells: a novel combination therapy. *Pathol Res Pract*. 2022;236:154004. doi:10.1016/j.prp.2022.154004
53. Chen L, Li H, Gao H, et al. Hsa_circ_0004194 suppresses colorectal cancer progression via hsa-miR-27a-3p. *Heliyon*. 2024;10(20):e39549. doi:10.1016/j.heliyon.2024.e39549
54. Hsieh AL, Walton ZE, J AB, et al. MYC and metabolism on the path to cancer. *Semin Cell Dev Biol*. 2015;43:11–21. doi:10.1016/j.semcdb.2015.08.003
55. Su Z, Liu Y, Wang L, et al. Regulation of SLC7A11 as an unconventional checkpoint in tumorigenesis through ferroptosis. *Genes Dis*. 2024;12(1):101254. doi:10.1016/j.gendis.2024.101254

56. Huang S, Wang Y, Xie S, et al. Hepatic TGFβr1 deficiency attenuates Lipopolysaccharide/D-Galactosamine-Induced acute liver failure through inhibiting GSK3β-Nrf2-Mediated hepatocyte apoptosis and ferroptosis. *Cell Mol Gastroenterol Hepatol*. 2022;13(6):1649–1672. doi:10.1016/j.jcmgh.2022.02.009
57. Zhou HM, Liu Y, Shi F, et al. CLK2 regulates the KEAP1/NRF2 and p53 pathways to suppress ferroptosis in colorectal cancer. *Cancer Res*. 2025;85(23):4734–4750. doi:10.1158/0008-5472.CAN-24-4949
58. Shang Y, Zhang J, Liu T. CAPG regulates doxorubicin resistance in hepatocellular carcinoma cells via TGFB1/Smad/Nrf2 signalling pathway. *J Cell Mol Med*. 2025;29(18):e70847. doi:10.1111/jcmm.70847